This article has been accepted for inclusion in a future issue of this journal. Content is final as presented, with the exception of pagination.

Measurement of Wave Near-Bed Velocity and Bottom Shear Stress by Ferrofluids

Rosaria Ester Musumeci, Vincenzo Marletta, Bruno Andò, *Senior Member, IEEE*
Salvatore Baglio, *Fellow, IEEE*, and Enrico Foti

***Abstract*— A novel direct measurement strategy of wave near-bed velocity and bottom shear stress based on the use of ferrofluids is presented. The proposed methodology is aimed at overcoming some of the limits of state-of-the-art instruments, for use in presence of both surface waves and sediments. An inductive readout strategy is proposed to sense displacements of the ferrofluid spike over the inductive circuit due to the flow. Experimental tests have been performed in a wave tank both in hydrostatic conditions and in the presence of regular linear waves corresponding to deep and intermediate water depth cases. Obtained results indicate the applicability of the proposed strategy also in the presence of suspended load (either moderate or intense) and of a moderate bed load transport.**

***Index Terms*— Bed velocity, bottom shear stress, ferrofluid, inductive readout, sediments, waves.**

I. Introduction

COASTAL erosion is a complex natural phenomenon produced by the combined action of waves, wind, tides, currents, ice, and other natural processes. Among these, waves represent one of the main driving forces of shoreline erosion [1], [2]. It is also expected that the effects of global warming will exacerbate the erosion of sandy beaches [3]. In this framework, the measurement of the near-bottom flow characteristics, particularly of the shear stresses and of the velocities, is crucial to correctly understand coastal processes, because at the sea bottom large flow resistances develop, strongly affecting both the flow hydrodynamics and the sediment transport [4]. The possibility to perform reliable measurements of shear stress is also needed for a number of aerodynamic studies [5], fluid dynamic monitoring [6], [7], diagnostics applications [8], underwater and biomedical applications [9], [10], research and industry [11] as well as to develop accurate modeling of these phenomenon [12], [13].

In the past, simple instruments, such as Preston tubes and Stanton tubes [14], have been used to measure bed shear stresses. However, because their application is restricted to flows where the normal law of the wall is valid, they are affected by several limits [15]. Nowadays, velocity measurements are often carried out using acoustic sensors, such as acoustic Doppler velocimetry [16] or optical sensors, such as laser Doppler velocimetry or particle image velocimetry systems [17], [18] and bottom shear stresses are indirectly derived from the logarithmic velocity profile, through the friction velocity. However, both acoustic and optical techniques cannot measure very close to the bottom, either due to the size of the sampling volume of the acoustic probe or to undesired reflection and disturbances from the bottom itself. Indeed, typically both kinds of instruments cannot provide measurements below 0.5 cm to the bottom. Furthermore, for example at the bottom of sea waves the velocity profiles are not logarithmic [19], [20].

Direct measurements of bed shear stresses can be performed by means of flush-mounted shear plates, which integrate the force over a relatively large area [21]. Besides other sources of errors, one of the main problem while using shear plates, is the tradeoff between sensor spatial resolution and the ability to measure small forces [22]. Another class of instruments is the one of thermal sensors, to which hot film anemometers belong [23]. Unfortunately, besides the well-known fragility of the sensors, hot film techniques are traditionally limited by difficulties in obtaining a unique calibration relationship between heat transfer and wall shear-stresses [24], from the reduction in sensitivity and complications in the dynamic response due to frequency-dependent conductive heat transfer into the substrate, and by measurement errors associated with mean temperature drift [25].

To overcome some of the above mentioned limits, Foti *et al.* [26] used bioluminescence to obtain maps of shear stress over the entire water column, though difficulties emerged in relation to the management of living sensors.

Andò *et al.* [27] and Musumeci *et al.* [28] demonstrated the possibility to use ferrofluids to measure near-bed velocity under two different controlled working conditions. In particular, investigations on the possibility to reconstruct velocity profiles by using ferrofluids and an image-processing procedure was presented in [27], and a new methodology based on an inductive readout circuit was presented in [28] along with preliminary quantitative validation in the steady-current case.

Following such two preceding seminal works, the characteristics of ferrofluids was exploited to perform quasi-noninvasive measurements of near-bed velocities and shear-stresses in the presence of waves and sediments and

Manuscript received June 20, 2014; revised August 7, 2014; accepted September 2, 2014. This work was supported in part by the European Commission through the Hydralab IV Project under Contract 261520 and in part by the Italian Ministry of Education, University and Research through the Projects of National Interest through the Hydrocar Project under Grant 20104J2Y8M_003. The Associate Editor coordinating the review process was Dr. Subhas Mukhopadhyay.

R. E. Musumeci and E. Foti are with the Department of Civil Engineering and Architecture, University of Catania, Catania 95124, Italy (e-mail: rmusume@dica.unict.it).

V. Marletta, B. Andò, and S. Baglio are with the Department of Electric, Electronic and Computer Sciences Engineering, University of Catania, Catania 95124, Italy (e-mail: bruno.ando@dieei.unict.it).

Digital Object Identifier 10.1109/TIM.2014.2359521

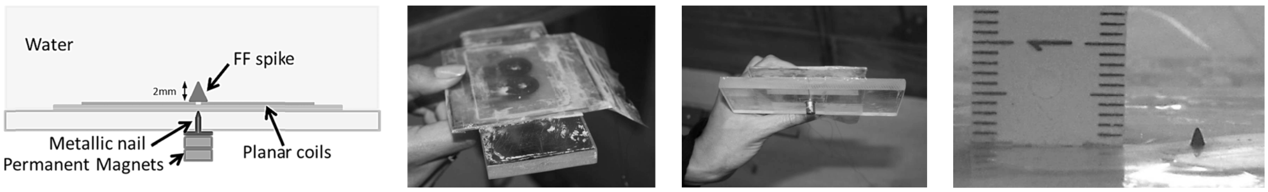

(a) (b) (c) (d)

Fig. 1. (a) Schematization of the setup used to generate the spike. (b) and (c) Real views of the setup. (d) Ferrofluid spike in hydrostatic conditions.

preliminary results were presented in [29]. The developed sensing system aims at overcoming some of the above limits such as use in the presence of surface waves, sediments, suspended load (either moderate or intense), and a moderate bed load transport, closeness to the wall and reduction of dimensions of the measuring area as well as minimization of the risk of perturbing the original flow conditions. With respect to the results presented in [29], in this paper a new optimized version of the conditioning electronic is proposed together with an extended analysis of the obtained experimental results. The new electronics makes it possible to setup the measurement system by removing the output voltage offset before starting a new measurement session with different initial conditions (different water levels). A new set of tests have been performed in a larger wave tank and quantitative results on the bottom shear stresses due to the wave motion are reported.

This paper is organized as follows: the proposed methodology, the setup, and the conditioning electronic are presented in Section II. Experimental results are discussed in Section III and conclusions are given in Section IV.

II. Proposed Methodology to Measure Wave Near-Bed Velocity and Bottom Shear Stress

Magnetic fluids belong to a multidisciplinary research area involving chemistry for the fluid synthesis, physics studying their behavior, basic theories and models, engineering which studies possible applications, and biology and medicine exploiting their applicability in the biomedical field [30], [31]. Ferrofluids are colloids of superparamagnetic nanoparticles stably dispersed in an organic nonmagnetic carrier liquid, usually oil or water [32], [33]. These nanomaterials manifest simultaneously fluid and magnetic properties. From a microscopic point of view, several mechanisms rule the interaction of paramagnetic nanoparticles such as attractive Van der Waals forces, thermal agitation, and anticohesion coatings [34], whereas from a magnetic point of view ferrofluids are characterized by a magnetism vector which follows the applied field without hysteresis. When a ferrofluid mass is subjected to an external magnetic field, its flat surface could become unstable and it shows a behavior ruled by the Rosensweig effect [34]. At certain intensity of the field, peaks appear at the fluid surface which typically form a static hexagonal pattern. Ferrofluids allows applications in several contexts: sealing for several industrial processes, loudspeakers, inertial dampers, angular position sensors, and computer disk drives are examples of applications where these materials have been widely adopted. An advantage in using magnetic fluids arises from the possibility to implement efficient, reliable, and robust against mechanical shocks sensors and actuators [35]–[46] thanks to the absence of mechanical moving parts and of solid-inertial masses and to the intrinsic feature to be shapeless. Another advantage of ferrofluid based sensors is the electrical insulation between the readout electronics and the liquid medium. This gives the possibility to easily control fluids and to implement measurements in liquids [29], [41]–[46].

In the proposed methodology to measure waves near-bed velocity and bottom shear stress, a tiny quantity of ferrofluid (order of 0.01 ml) is located at the wall and subject to a permanent magnetic field to generate a single small ferrofluid spike (by exploiting the Rosensweig effect) with a conical shape with an height of about 2 mm. The spike height fixes the responsivity of the sensing setup. Actually, higher spikes increases the setup responsivity, but on the other hand the higher the peak, the narrower the operating range because higher velocities in the upper part can remove the ferrofluid spike or part of it. To avoid this problem, the magnetic retaining force exerted by the permanent magnets should be increased thus to obtain a stiffer spike. However, as a consequence, stiffer spikes move the operating range toward higher near-bed velocities reducing in turn the responsivity of the system to lower velocities. It follows that a compromise must be found. The spike having an height of 2 mm, has been experimentally found to provide a good compromise between the responsivity of the sensing circuit in the range of velocities of interest and the need of measurements very close to the bottom.

A schematization of the setup used to generate the spike is shown in Fig. 1(a): the ferrofluid drop is located in the middle between two copper planar coils. A polyethylene terephthalate substrate with a thickness of about 100 μm was used to cover the planar coils to electrically isolate the coils from the water and the ferrofluid drop. The printed circuit board is glued onto a Perspex plate about 1 cm thick which in the case of movable bottom experiments contrast buoyancy or drag effects on the coils and can be easily buried within the sand. One or more permanent magnets are used to generate the ferrofluid spike and to maintain the position of the ferrofluid drop at the measuring station. To obtain a single spike shape, a metallic nail is used to concentrate the magnetic field lines. Moreover, the use of a Perspex plate allows to reproduce also in the presence of a sandy bottom the same geometric distances between the ferrofluid, coils, and permanent magnets, as in the case of fixed bottom experiments [28].

Real views of the setup and ferrofluid spike are shown in Fig. 1(b)–(d),

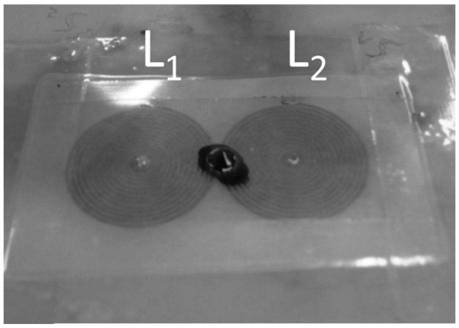

Fig. 2. Two planar coils used to sense the deformation of the ferrofluid spike placed in the middle of the coils.

The commercial ferrofluid EFH1 produced by Ferrotec has been used. Because it is specifically designed for educational purposes, hazard for human health and the environment are reduced. The only caution we used were protective gloves to avoid repeated skin contact. During the experiments the waste of the ferrofluid was treated according to the National laws on disposal of waste oils.

Being immiscible with water, in hydrostatic conditions the ferrofluid spike remains where it has been generated. In dynamic conditions, under the action of the external water flow, the ferrofluid undergoes deformation and displacement in the direction of the flow. Considering the rheological properties of the ferrofluid and the dynamic equilibrium of the ferrofluid spike, it can be shown that the deformation of the ferrofluid in the flow direction is related to the bottom shear stresses [27], [28]. By sensing the deformation of the ferrofluid spike, the characteristics of the flow very close to the bottom can be measured. As it will be more clear in the following, because the position of the ferrofluid spike is controlled only by the intensity of the magnetic field and by the action of the flow, the proposed technique is designed to overcome some of the limits of the available instrumentation, and it can be also used in the presence of sediments without damages to the measuring system. To detect the displacement of the center of mass of the ferrofluid spike induced by the flow, an inductive read-out strategy was proposed [29].

Such a strategy uses two photolitographically engraved copper planar coils connected to a suitable conditioning circuit. The ferrofluid spike sits initially at the center of the two coils as shown in Fig. 2.

The movement of the ferrofluid spike produces a variation in the magnetic permeability μ and consequently a variation of the inductance L of the coils. Therefore the displacement can be sensed by the two planar coils, because the perturbation of the magnetic field generated by the displacement of the spike is transduced in a voltage variation by a suitable conditioning circuit.

A schematization of the conditioning circuit is shown in Fig. 3. Essentially it consists of an ac bridge, a differential amplifier, and a rectifier and filters to have a dc output voltage. The ac bridge was driven by a sinusoidal voltage signal provided by a waveform generator HP33120A and an operational amplifier TL081 (STMicroelectronics) in a buffer configuration. An instrumentation amplifier INA111AP (Burr Brown) has been used to amplify the variation of the bridge output voltage.

Although main information about the displacement of the center of mass of the ferrofluid due to the flow could be obtained by the output at this stage of the conditioning circuit (the bridge + the differential amplifier), a more complex electronic has been developed to avoid the need to use a more performant data acquisition instrumentation. Actually, the ac bridge used to convert the variation of L in an voltage variation, was driven by a sinusoidal voltage signal at 100 kHz which requires a very high sampling frequency in the order of megahertz. By using a dc output conditioning circuit this sampling frequency can be drastically reduced and consequently low-cost Data AcQuisition (DAQ) boards can be used. Moreover, the use of a lower sampling frequency reduces the efforts for both the data storage and data analysis. To this aim, a full wave rectifier and a low-pass filter to remove the ripple from the rectified signal have been employed. In the new version of the conditioning electronic a differential amplifier which acts as an adjustable subtractor has been added to remove the static offset from the output voltage signal from the filter.

With a variable resistor (a trimmer) it is possible to adjust the level of the subtractor output signal. As already stated, this makes it possible to setup the measurement system by removing the output voltage offset before starting a new measurement session with different initial water-level conditions. Actually a relationship between the water level in static conditions and the output voltage of the circuit has been observed [29] and investigated. A modeling of this relationship is presented in the following section.

Finally, a further active low-pass filter amplifies the variations of the subtractor output voltage due to the displacement of the ferrofluid spike and filter possible high frequency noises. The value of the output dc signal is proportional to the displacement of the ferrofluid spike due to the flow.

III. Experimental Campaign

The experiments have been carried out at the Hydraulic Laboratory of the University of Catania.

Preliminary investigations on the effect of water-level variations on the output voltage of the circuit have been performed in static conditions by changing the level h of water in a tank where the planar coils were placed at the bottom over a sand base. To assess the behavior of the conditioning circuit and its sensitivity to changes of the water depth, the tests have been carried out over a large range of water depths, $h = 0-60$ cm. To avoid saturation of the output voltage signal, V_{out}, each test was carried out with a different offset of the circuit. Moreover, the effects of the different intensities of the magnetic field was also assessed by using two or four permanent neodymium disc magnets type S0805N [47]. The same magnets have been used during the dynamic experiments. Main technical information about this type of magnets are reported in Table I [47].

An example of the experimental results in cases of: 1) no magnets and no ferrofluid; 2) presence of two magnets and no ferrofluid; 3) presence of four magnets and no ferrofluid; and 4) four magnets and ferrofluid is shown in Fig. 4.

This article has been accepted for inclusion in a future issue of this journal. Content is final as presented, with the exception of pagination.

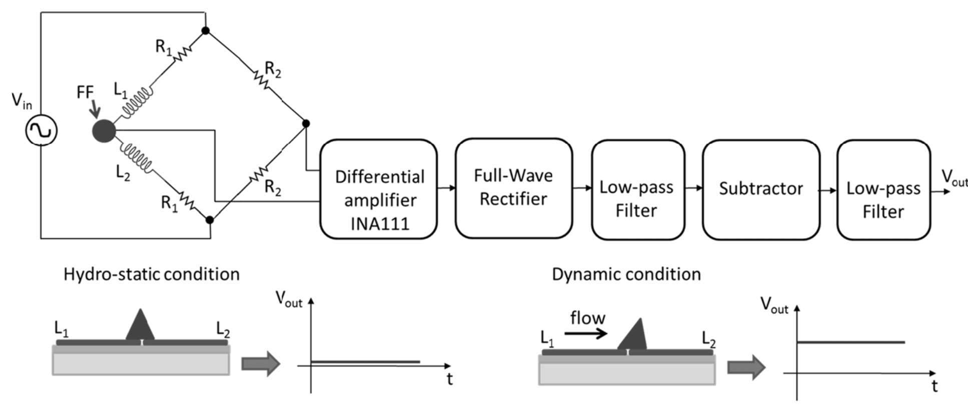

Fig. 3. Conditioning circuit schematization and working principle.

TABLE I
TECHNICAL DATA OF THE MAGNETS S0805N

Shape	Disc
Diameter	8 mm
Height	5 mm
Direction of magnetization	Axial (parallel to height)
Material	NdFeB (Neodymium Iron Boron)
Type of coating	Nickel (Ni-Cu-Ni)
Strength	approx. 19.9 N
Magnetisation (Grade)	N45

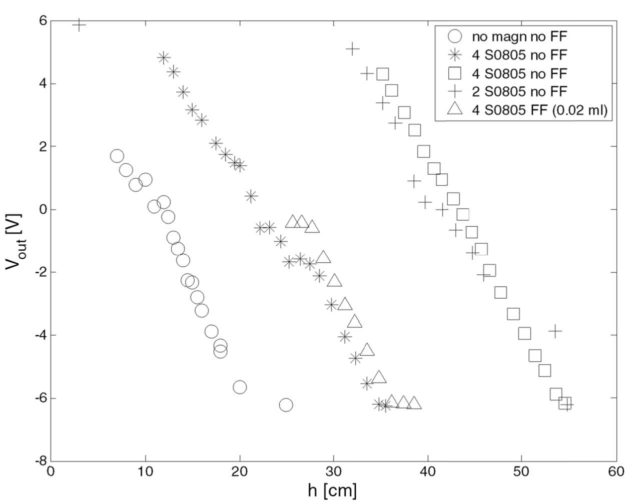

Fig. 4. Experimental results on the effects of hydrostatic changes of the water depth on the output voltage of the conditioning circuit.

It appears that the relationship between hydrostatic changes of the water depth Δh and changes in the output voltage ΔV_{out} is linear and it is independent on the presence of the ferrofluid and on the intensity of the controlling magnetic field. The following linear relationship has been derived:

$$\Delta h = -1.81 \Delta V_{\text{out}}. \quad (1)$$

Concerning the measurements at the bottom of regular surface waves, a first series of tests was carried out in a wave flume which is 9-m long, 0.5-m wide, and 0.7-m high.

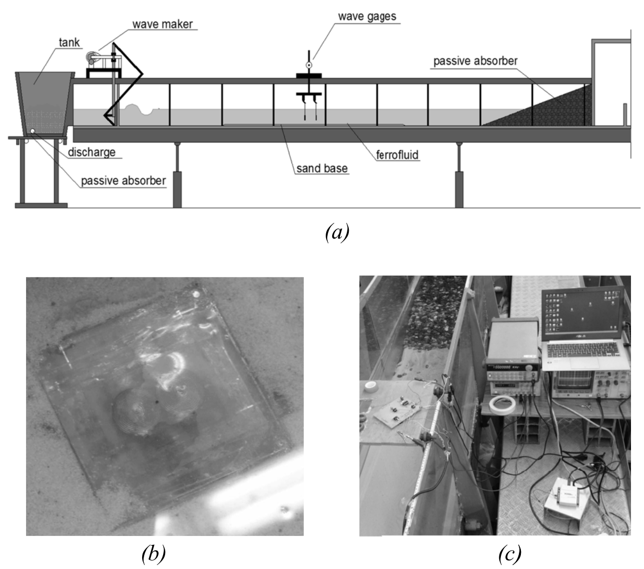

Fig. 5. (a) Section of the wave flume. (b) Planar coils with the ferrofluid located at the center. (c) Conditioning circuit and acquisition system [29].

A schematization of the flume in shown in Fig. 5(a) [29]. In the central part of the flume a 4-cm thick layer of sand is present, whose grains have a median diameter d_{50} equal to 0.56 mm.

The permanent magnets are buried within the sand, while the two coils with the ferrofluid are located at the bed level [Fig. 5(b)]. Note that the ferrofluid height is of the same order of magnitude of the sand grains. The conditioning circuit is positioned outside of the flume [Fig. 5(c)] [29]. The voltage output of the system is monitored using an oscilloscope and the data are digitally acquired by an NI 6009-USB DAQ board.

Linear monochromatic waves have been generated using a piston-type wavemaker with wave heights H in the range 1.1–6.2 cm and wave periods T in the range 0.50–2.2 s. The water depth h was in the range 21.8–22.5 cm. The wave characteristics have been chosen to cover the range of deep and intermediate water waves. For the sake of completeness, measurements of surface elevation and of velocity profiles are obtained through resistive wave gauges and a 16 MHz micro-ADV, respectively. Such data allow velocity and bottom shear stresses to be extrapolated from wave bottom boundary layer theory.

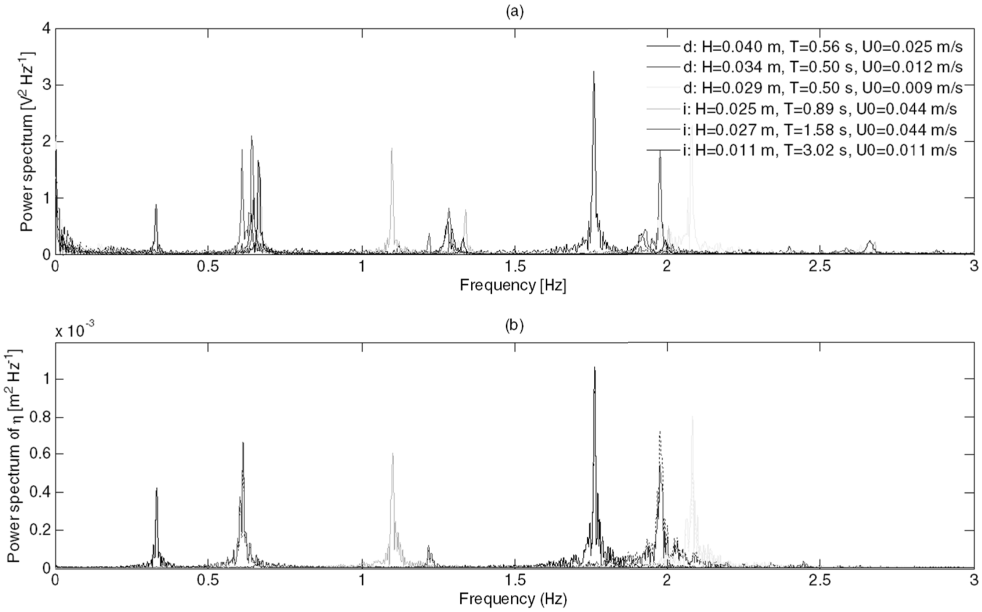

Fig. 6. Power spectra of (a) measured output voltage of the circuit and (b) surface elevation obtained by reference instrumentation [29].

Fig. 6 shows a comparison between the power spectra of the output voltage of the proposed system and the power spectra of the surface elevation obtained by the reference instrumentation [29]. The legend indicates the deep water wave (d) and intermediate water wave conditions (i). Moreover, also the wave height H, the wave period T, and the bottom velocity U_0 evaluated according to linear theory are shown. In particular, in the top and the bottom frames as shown in Fig. 6 measurements corresponding to the same wave conditions are plotted using lines of the same color.

From the analysis of the experimental data, it clearly appears that in the case of an oscillating motion, the system is able to properly react to the different wave frequencies, because the first harmonics has the same frequency both in the developed circuit output signal and in the reference wave gauge signal.

Moreover, Fig. 6 shows that also the intensities of the output voltage and of the wave measurements are consistent (i.e., more energetic higher waves have larger output voltage).

It can be noticed that spurious peaks appears in the measured output voltage of the circuit at frequency of about 0.7 Hz. Such peaks are due to the presence of the couple of resistive wave gauges used to measure the surface elevation and can be easily filtered out. From such preliminary results, it follows that it is possible to effectively extend the technique from steady-current to wave conditions also in the presence of sediments.

To confirm such a result, a new series of test has been carried out in another wave tank, which is 18-m long, 3.6-m wide, and 1.0-m high (Fig. 7). A peculiarity of such a tank is that a wider range of water depths and wave conditions can be tested compared with the previous one. Also in this case the two planar coils along with the permanent magnets have been located in a sandy bottom with $d_{50} = 0.56$ mm and the ferrofluid spike has been generated at the center of the two planar coils. It should be noticed that the axis of the coils has been carefully aligned with the direction of the flow. Measurements

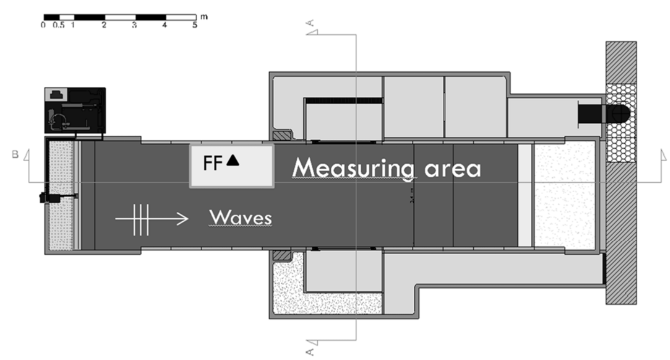

Fig. 7. Plan view of the larger wave flume and location of the measuring area with the ferrofluid.

of the surface elevation and of the ferrofluid deformations have been obtained by means of resistive wave gauges and of the conditioning circuit described above. Experimental tests have been carried out both in hydrostatic conditions and in the presence of regular linear waves, which have been generated with wave heights H ranging in the interval 0.4–6.2 cm and wave period T in the range 0.20–1.04 s. During this campaign, the water depth h was 0.25 cm in all the tests. Also in this test series, we have obtained both deep and intermediate water depth conditions.

An analysis of the frequency response of the proposed measuring system based on independent measurements of the period of the surface waves obtained through the wave gauges, is shown in Fig. 8 where T_{circ} and T_{wave} indicate the wave periods estimated by the measurements of the conditioning circuit and of the wave gauges, respectively. Several conditions of the controlling permanent magnetic field have been considered. It can be noticed that the frequency response of the system is linear, with a better behavior in intermediate water depth conditions, where the interaction of the wave motion with the bottom is stronger. Some dispersion of the data is observed in the presence of deep water conditions, particularly for smaller wave heights and periods.

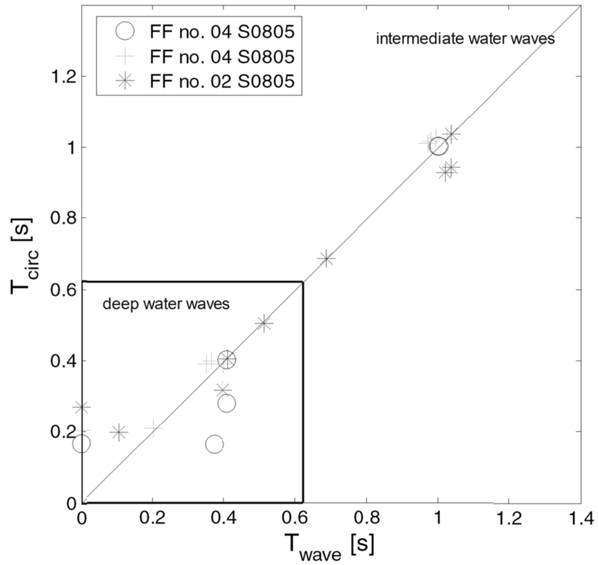

Fig. 8. Frequency response of the proposed measuring system in terms of the wave period measured by the wave gauges.

The wavelength L, the amplitude of velocity in the core region at the bottom of the flow U_0, the amplitude of the wave oscillations A have been obtained from the measured wave characteristics H, T and h, by applying linear wave theory. Then, from wave boundary layer theory, the thickness of the bottom boundary layer $\delta = (\nu/2\sigma)^{1/2}$ has been calculated along with the time-dependent velocity profiles

$$u(y) = U_0 \sin \sigma t - e^{-\frac{y}{\sqrt{\frac{2\nu}{\sigma}}}} \sin\left(\sigma t - \frac{y}{\sqrt{\frac{2\nu}{\sigma}}}\right) \quad (2)$$

with y being the vertical coordinate, $\sigma = 2\pi/T$ the angular frequency and ν the kinematic viscosity. Fig. 9 shows a typical behavior of such time-varying theoretical velocity profiles. Fig. 9 also shows how such velocity profiles have been used to estimate the velocity υ_{xFF} as the maximum velocity in the correspondence of the ferrofluid location. Finally, such velocity υ_{xFF} is considered to calibrate the measuring system in the presence of waves.

Example of calibration curves, that is, of the relationship between the maximum velocity in the correspondence of the ferrofluid spike υ_{xFF} and the peak output voltage recovered by the conditioning circuit V_{pp} are shown in Fig. 10. Here, both the calibration obtained with the raw data and that obtained by applying the correction to the data to account for the sensitivity of the measuring system to changes in the water depth are reported. The effect of the water-level correction induces mainly an offset of the data. It may be noticed that, as in the case of steady-flow condition described in Section II, the calibration curve appears again to possess a parabolic shape, which is more evident with a less strong magnetic force (no. 2 S0805 magnets). Because the relationship between υ_{xFF} and V_{pp} should be bijective, it should be noticed the measuring system cannot be used to measure velocities in the low-velocity region ($\upsilon_{xFF} < 4$ cm/s). The latter result is in agreement with the results obtained in the steady-flow conditions [28].

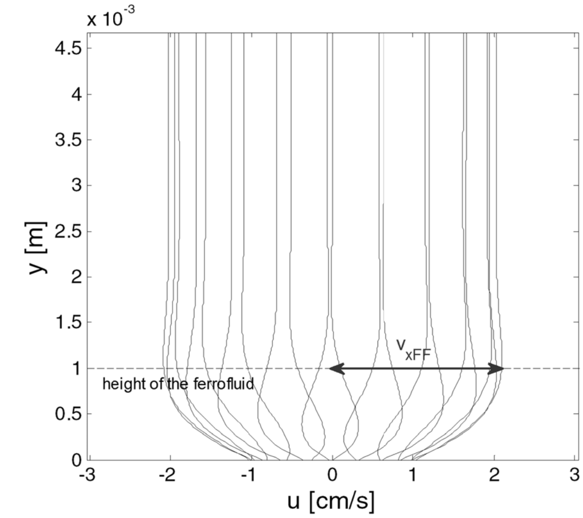

Fig. 9. Wave boundary layer velocity profile used to estimate the velocity in the correspondence of the ferrofluid sensor.

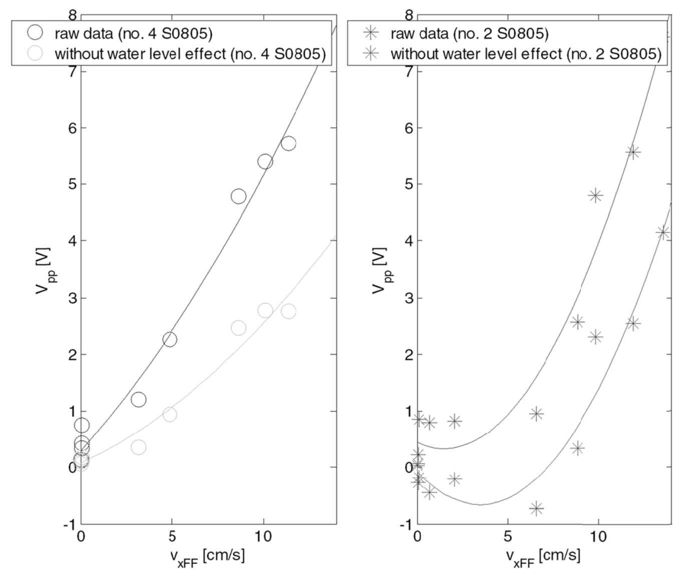

Fig. 10. Experimental parabolic relationship between the peak output voltage and the maximum near-bottom mean velocity in the presence of waves. The correction of the peak output voltage as a function of the water level change is also reported.

According to [48], a conventional form of the maximum bottom shear stress in an oscillatory flow can be written as

$$\tau_{\max} = \frac{\rho f}{8} U_0 \left| U_0 \right| \quad (3)$$

with ρ being the water density and where the friction factor f can be estimated in laminar conditions as

$$f = \frac{8}{\mathrm{Re}^{1/2}} \quad (4)$$

with the Reynolds number expressed as

$$\mathrm{Re} = \frac{U_0 A}{\nu}. \quad (5)$$

Fig. 11 shows two experimental relationships between the peak output voltage and the maximum bottom shear stress in the presence of waves, obtained using different intensities of the controlling magnetic field. In analogy with the

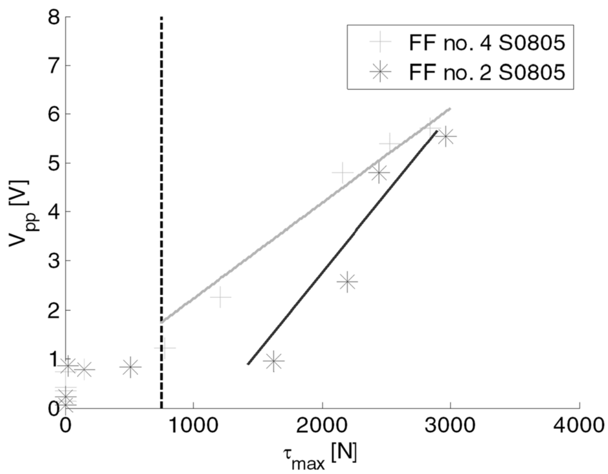

Fig. 11. Experimental relationship between the peak output voltage and the maximum bottom shear stress in the presence of waves. Two solid colored lines: two different intensity of the controlling permanent magnetic field. Black dashed line: minimum measurable maximum bottom shear stress.

results on the near-bed velocity discussed previously (Fig. 10), a minimum measurable bottom shear stress exists, whose value is shown by the dashed line in Fig. 11. It can be noticed that the behavior of the proposed measuring system is linear in the field of interest. It can also be observed that the sensitivity of the developed sensor increases as the intensity of the external magnetic field decreases. This is due to the fact that a larger magnetic force generate a stiffer ferrofluid spike which feels less the action of the flow. Obviously, also the inferior limits of v_{xFF} or of $\tau_{\max}$ are function of the controlling magnetic force. It follows that the choice of such a force must be performed depending on the range of the near-bed velocities or of bottom shear stresses to be measured.

IV. Conclusion

In this paper, a novel direct measurement strategy to measure wave near-bed velocity and bottom shear stresses according to the use of ferrofluids has been presented. The proposed methodology is based on the use of a ferrofluid spike, generated at the bottom through the use of permanent magnets, which is deformed because of the action of the water flow. Therefore, by sensing such a deformation it is possible to determine flow velocities and shear stresses very close to the bottom. An inductive readout strategy is proposed to sense displacements of the ferrofluid spike. The proposed methodology is aimed at overcoming some of the limits of state-of-the-art instruments, for use in presence of surface waves, suspended load (either moderate or intense), and a moderate bed load transport. Others main outcomes of the proposed methodology are reduction of dimensions of the measuring area and minimization of the risk of perturbing the original flow conditions. Experimental tests have been performed in a wave tank both in hydrostatic conditions and in the presence of regular linear waves with different wave heights corresponding (compared with the water depth) to deep and intermediate water depth cases. Quantitative results on the bottom shear stresses due to the wave motion have been discussed. Obtained results indicate the applicability of the proposed strategy also in presence of suspended impurities (either moderate or intense) and of a moderate bed sediments transport.

References

[1] E. L. Gallagher, S. Elgar, and R. T. Guza, "Observations of sand bar evolution on a natural beach," *J. Geophys. Res. C, Oceans*, vol. 130, no. C2, pp. 3203–3215, 1998.

[2] T. Butt and P. Russel, "Hydrodynamics and cross-shore sediment transport in the swash-zone of natural beaches: A review," *J. Coastal Res.*, vol. 16, no. 2, pp. 255–268, 2000.

[3] K. Zhang, B. C. Douglas, and S. P. Leatherman, "Global warming and coastal erosion," *Climatic Change*, vol. 64, no. 1–2, pp. 41–58, 2004.

[4] R. Soulsby, *Dynamics of Marine Sands: A Manual for Practical Applications*. London, U.K.: Thomas Telford Publications, 1997.

[5] F. Jiang *et al.*, "Flexible shear stress sensor skin for aerodynamics applications," in *Proc. 13th IEEE Int. Conf. Micro Electro Mech. Syst. (MEMS)*, Miyazaki, Japan, Jan. 2000, pp. 364–369.

[6] A. Huang, J. Lew, Y. Xu, Y.-C. Tai, and C.-M. Ho, "Microsensors and actuators for macrofluidic control," *IEEE Sensors J.*, vol. 4, no. 4, pp. 494–502, Aug. 2004.

[7] H. Yu, L. Ai, M. Rouhanizadeh, D. Patel, E. S. Kim, and T. K. Hsiai, "Flexible polymer sensors for in vivo intravascular shear stress analysis," *IEEE J. Microelectromech. Syst.*, vol. 17, no. 5, pp. 1178–1186, Oct. 2008.

[8] G. Soundararajan, T. K. Hsiai, L. DeMaio, M. Chang, and S. Chang, "MEMS shear stress sensors for cardiovascular diagnostics," in *Proc. 26th Annu. Int. Conf. IEEE Eng. Med. Biol. Soc. (IEMBS)*, vol. 1. Sep. 2004, pp. 2420–2423.

[9] Y. Xu *et al.*, "Micromachined thermal shear-stress sensor for underwater applications," *IEEE J. Microelectromech. Syst.*, vol. 14, no. 5, pp. 1023–1030, Oct. 2005.

[10] L. Ai, H. Yu, W. Dai, S. L. Hale, R. A. Kloner, and T. K. Hsiai, "Real-time intravascular shear stress in the rabbit abdominal aorta," *IEEE Trans. Biomed. Eng.*, vol. 56, no. 6, pp. 1755–1764, Jun. 2009.

[11] D. T. Fisher, S. A. Clayton, D. V. Boger, and P. J. Scales, "The bucket rheometer for shear stress-shear rate measurement of industrial suspensions," *J. Rheol.*, vol. 51, no. 5, pp. 821–831, 2007.

[12] L. Cavallaro, P. Scandura, and E. Foti, "Turbulence-induced steady streaming in an oscillating boundary layer: On the reliability of turbulence closure models," *Coastal Eng.*, vol. 58, no. 4, pp. 290–304, 2011.

[13] C. Lo Re, R. E. Musumeci, and E. Foti, "A shoreline boundary condition for a highly nonlinear Boussinesq model for breaking waves," *Coastal Eng.*, vol. 60, pp. 41–52, Feb. 2012.

[14] M. R. Head and I. Rechenberg, "The Preston tube as a means of measuring skin friction," *J. Fluid Mech.*, vol. 14, no. 1, pp. 1–17. 1962.

[15] M. P. Escudier and M. Acharya, "Critique of the computational Preston tube method," *Experim. Fluids*, vol. 5, no. 1, pp. 59–65, 1987.

[16] R. E. Musumeci, L. Cavallaro, E. Foti, P. Scandura, and P. Blondeaux, "Waves plus currents crossing at a right angle: Experimental investigation," *J. Geophys. Res.*, vol. 111, no. C7, pp. C07019-1–C07019-19, 2006.

[17] D. T. Cox, N. Kobayashi, and A. Okayasu, "Bottom shear stress in the surf zone," *J. Geophys. Res., Oceans (1978–2012)*, vol. 101, no. C6, pp. 14337–14348, Jun. 1996.

[18] W. N. Smith, P. Asavapranee, J. Katz, and T. Osborn, "PIV measurements in the bottom boundary layer of the coastal ocean," *Experim. Fluids*, vol. 33, no. 6, pp. 962–971, 2002.

[19] M. A. Abdelrhman and K. W. Bedford, "Recognition of spatial structures and ensemble averages in the benthic boundary layer," *J. Geophys. Res.*, vol. 92, no. C11, pp. 11825–11844, 1987.

[20] L. Cavallaro, P. Scandura, and E. Foti, "Turbulence-induced steady streaming in an oscillating boundary layer: On the reliability of turbulence closure models," *Coastal Eng.*, vol. 58, no. 4, pp. 290–304, 2011.

[21] H. P. Riedel, J. W. Kamphuis, and A. Brebner, "Measurement of bed shear stress under waves," in *Proc. 13th Conf. Coastal Eng.*, Vancouver, BC, Canada, 1972, pp. 587–603.

[22] K. G. Winter, "An outline of the techniques available for the measurement of skin friction in turbulent boundary layers," *Prog. Aerosp. Sci.*, vol. 18, no. 1, pp. 1–57, 1977.

[23] B. M. Sumer, M. M. Arnskov, N. Christiansen, and F. E. Jorgensen, "Two-component hot-film probe for measurements of wall shear stress," *Experim. Fluids*, vol. 15, no. 6, pp. 380–384, Oct. 1993.

[24] M. P. Barnes and T. E. Baldock, "Direct bed shear stress measurements in laboratory swash," *J. Coastal Res.*, vol. 50, pp. 641–645, Apr. 2007.
[25] J. W. Naughton and M. Sheplak, "Modern developments in shear-stress measurement," *Prog. Aerosp. Sci.*, vol. 38, nos. 6–7, pp. 515–570, 2002.
[26] E. Foti, C. Faraci, R. Foti, and G. Bonanno, "On the use of bioluminescence for estimating shear stresses over a rippled seabed," *Meccanica*, vol. 45, no. 6, pp. 881–895, 2010.
[27] B. Andò, S. Baglio, C. Trigona, and C. Faraci, "Ferrofluids for a novel approach to the measurement of velocity profiles and shear stresses in boundary layers," in *Proc. IEEE Sensors*, Oct. 2009, pp. 1069–1071.
[28] R. E. Musumeci, V. Marletta, C. Faraci, B. Andò, S. Baglio, and E. Foti, "Measurement of bottom velocities and shear stresses through ferrofluid," in *Proc. 35th IAHR World Congr.*, Chengdu, China, Sep. 2013, pp. 1–8.
[29] B. Andò, S. Baglio, V. Marletta, R. E. Musumeci, and E. Foti, "Measurement of bottom velocities and shear stresses by ferrofluids at the sea bottom," in *Proc. IEEE Int. Instrum. Meas. Technol. Conf. (I2MTC)*, May 2014, pp. 1–4.
[30] B. Andò, S. Baglio, and A. Beninato, "Magnetic fluids for biomedical application," in *Advances in Biomedical Sensing, Measurements, Instrumentation and Systems* (Lecture Notes in Electrical Engineering), vol. 55, S. C. Mukhopadhyay and A. Lay-Ekuakille, Eds. Berlin, Germany: Springer-Verlag, 2010, pp. 16–28.
[31] Q. A. Pankhurst, J. Connolly, S. K. Jones, and J. Dobson, "Applications of magnetic nanoparticles in biomedicine," *J. Phys. D, Appl. Phys.*, vol. 36, no. 13, pp. 167–181, 2003.
[32] R. E. Rosensweig, *Ferrohydrodynamics*. New York, NY, USA: Cambridge Univ. Press, 1985.
[33] S. W. Charles, "The preparation of magnetic fluids," in *Ferrofluids: Magnetically Controllable Fluids and Their Applications* (Lecture Notes in Physics). Berlin, Germany: Springer-Verlag, 2002, pp. 3–18.
[34] E. L. Resler, Jr., and R. E. Rosensweig, "Magnetocaloric power," *AIAA J.*, vol. 2, no. 8, pp. 1418–1422, 1964.
[35] G. Q. Hu and W. H. Liao, "A feasibility study of a microaccelerometer with magnetorheological fluids," in *Proc. IEEE Int. Conf. Robot., Intell. Syst. Signal Process.*, Hunan, China, Oct. 2003, pp. 825–830.
[36] R. Olaru and D. D. Dragoi, "Inductive tilt sensor with magnets and magnetic fluid," *Sens. Actuators A, Phys.*, vol. 120, no. 2, pp. 424–428, Feb. 2005.
[37] A. Hatch, A. E. Kamholz, G. Holman, P. Yager, and K. F. Böhringer, "A ferrofluidic magnetic micropump," *J. Microelectromech. Syst.*, vol. 10, no. 2, pp. 215–221, Jun. 2001.
[38] H. Hartshorne, C. J. Bakhouse, and W. E. Lee, "Ferrofluid-based microchip pump and valve," *Sens. Actuators B, Chem.*, vol. 99, nos. 2–3, pp. 592–600, May 2004.
[39] C. Yamahata, M. Chastellain, V. K. Parashar, A. Petri, H. Hofmann, and M. A. M. Gijs, "Plastic micropump with ferrofluidic actuation," *J. Microelectromech. Syst.*, vol. 14, no. 1, pp. 96–102, Feb. 2005.
[40] B. Andò, A. Ascia, S. Baglio, and N. Pitrone, "Magnetic fluids and their use in transducers," *IEEE Mag. Instrum. Meas.*, vol. 9, no. 6, pp. 44–47, Nov. 2006.
[41] B. Andò, S. Baglio, A. Beninato, and V. Marletta, "Ferrofluids and their use in sensors," in *Smart Sensors for Industrial Applications*, K. Iniewski, Ed. Boca Raton, FL, USA: CRC Press, 2013, pp. 355–368.
[42] B. Ando, A. Ascia, and S. Baglio, "A ferrofluidic inclinometer in the resonant configuration," *IEEE Trans. Instrum. Meas.*, vol. 59, no. 3, pp. 558–564, Mar. 2010.
[43] B. Ando, A. Ascia, S. Baglio, and A. Beninato, "A ferrofluidic inertial sensor exploiting the Rosensweig effect," *IEEE Trans. Instrum. Meas.*, vol. 59, no. 5, pp. 1471–1476, May 2010.
[44] B. Ando, S. Baglio, and A. Beninato, "An IR methodology to assess the behavior of ferrofluidic transducers—Case of study: A contactless driven pump," *IEEE Sensors J.*, vol. 11, no. 1, pp. 93–98, Jan. 2011.
[45] B. Andò, S. Baglio, and A. Beninato, "Path driving of ferrofluid samples for bio-sensing applications," in *Proc. IEEE Int. Instrum. Meas. Technol. Conf. (I2MTC)*, May 2012, pp. 290–293.
[46] B. Andò, S. Baglio, and A. Beninato, "A low-cost inertial sensor based on shaped magnetic fluids," *IEEE Trans. Instrum. Meas.*, vol. 61, no. 5, pp. 1231–1236, May 2012.
[47] Supermagnete. *Datasheet Article S-08-05-N*. [Online]. Available: http://www.supermagnete.it/eng/data_sheet_S-08-05-N.pdf, accessed Sep. 9, 2014.
[48] R. G. Dean and R. A. Dalrymple, "Water wave mechanics for engineers and scientists," *Advanced Series on Ocean Engineering*, vol. 2. Singapore: World Scientific, 1991.

Rosaria Ester Musumeci received the Ph.D. degree in hydraulic engineering from the University of Catania, Catania, Italy.

She has been with the Department of Civil Engineering and Architecture, University of Catania, since 2003, where she is currently an Assistant Professor. She is involved in several European and national research projects. Her current research interests include coastal engineering and the development of innovative instruments for use in hydraulic laboratories.

Vincenzo Marletta received the M.S. and Ph.D. degrees from the University of Catania, Catania, Italy, in 2007 and 2011, respectively.

He is currently a Temporary Research Fellow with the Department of Electric, Electronic and Information Engineering, University of Catania. His current research interests include sensor design and characterization, smart materials, inkjet printed sensors, energy harvesting, multisensor architectures for environmental monitoring and AAL, nonlinear signal processing, and exploitation of nonlinear dynamics in sensors.

Bruno Andò (M'97–SM'13) was born in Catania, Italy, in 1969. He received the M.S. degree in electronic engineering and the Ph.D. degree in electrical engineering from the University of Catania, Catania, in 1994 and 1999, respectively.

He has been with the Department of Electric, Electronic and Information Engineering, University of Catania, since 1999, where he is currently an Associate Professor of Sensors and Advanced Instrumentation. His current research interests include sensors design and optimization, inkjet printed sensors, energy harvesting, smart materials, multisensor architectures for environmental monitoring and AAL, and nonlinear signal processing.

Salvatore Baglio Baglio (M'95–SM'03–F'12) was born in Catania, Italy, in 1965. He received the Laurea and Ph.D. degrees from the University of Catania, Catania, in 1990 and 1994, respectively.

He has been with the Department of Electric, Electronic and Information Engineering, University of Catania, since 1996, where he is currently an Associate Professor of Electronic Instrumentations and Measurements. His current research interests include measurement methodologies, smart sensors, microsensors, and microsystems.

Dr. Baglio is an Associate Editor of the IEEE TRANSACTIONS ON INSTRUMENTATION AND MEASUREMENTS.

Enrico Foti received the Ph.D. degree in hydrodynamics from the University of Padua, Padua, Italy, in 1994.

He has been with the University of Catania, Catania, Italy, since 1994, and a Full Professor of Hydraulics since 2003. He is currently responsible of numerous European Union-funded research projects. His current research interests include small-scale coastal morphodynamics, turbulence, hydraulic risks, wave energy, and development of innovative instruments to be used in hydraulic laboratories.